

Short communication

Flash grain welding in yttria stabilized zirconia

Reginaldo Muccillo^a, Michel Kleitz^{b,*}, Eliana N.S. Muccillo^a

^a Center of Science and Technology of Materials, Energy and Nuclear Research Institute - IPEN, Travessa R 400, Cidade Universitaria, S. Paulo, SP 05508-900, Brazil

^b Laboratory of Electrochemistry and Physicochemistry of Materials and Interfaces LEPMI, Polytechnique Institute of Grenoble, 1130 Rue de la Piscine BP 75, 38402 St Martin d'Herès, France

Received 27 January 2011; received in revised form 14 February 2011; accepted 18 February 2011

Abstract

Self-standing samples made of isostatically pressed powders of $\text{ZrO}_2:8 \text{ mol\% Y}_2\text{O}_3$ were submitted to AC signals of 60 and 1000 Hz. At temperatures of around 900 °C, a current density exceeding approximately 100 mA/cm² starts an avalanche process with a fast increasing current under constant voltage. It lasts about 60 s and it is preceded by an induction period of the order of 30 s. After that, the material is sintered as confirmed by impedance diagrams. Relative densities of 94% could be obtained.

© 2011 Elsevier Ltd. All rights reserved.

Keywords: A. Sintering; B. Grain boundaries; C. Impedance; C. Ionic conductivity; D. ZrO_2

1. Introduction

In addition to obvious economical and technical incitements, the search for fast sintering techniques has been accelerated by the upsurge of an overwhelming interest in nanostructured materials. It is well established that fast sintering can be achieved without any substantial grain growth. This is the case with solid oxide ion conductors such as stabilized zirconia and doped ceria. Industrial equipment based on the spark plasma sintering (SPS) is commonly used for this purpose. Five recent review papers^{1–5} give extensive details on the fast sintering techniques (also called electric current activated/assisted sintering technique – ECAS,² current-activated, pressure-assisted densification – CAPAD⁴ or pulsed electric current sintering – PECS⁵) which have been applied to a large variety of materials. Dense, nanograined yttria stabilized zirconias have been successfully obtained using the SPS technique with commercial and improved equipments.^{6,7} More theoretically oriented studies^{8–12} of the oxide sintering mechanisms have recently shown that a DC or AC voltage applied during a conventional sintering process lowers the densification temperature by inhibiting the grain growth. A flash sintering of nanograin TZP has also been observed under DC polarization.¹³

Referring to fairly systematic investigations of the blocking of the ionic carriers by various microstructure defects in YSZ,^{14,15} it has been concluded that the major part of the material resistance of a porous sample is located at the contacts between the grains. Therefore, applying a voltage to such a porous material will mainly generate a Joule effect at the contacts between the grains. It is likely to favor their welding. The analogy with the metal spot-welding may be misleading, but gives an image of the local heating effect at the microstructure level. Another common observation in the impedance characterization of the sintered oxide ion conductors is that contacts between the grains in the sintered bodies are also characterized by fairly important electric capacitances. Passing an AC current through such contacts would charge and discharge these capacitances and therefore move back and forth the adjoining ions which are the electric carriers. Under high AC current, this is likely to result in a heavy shuffling of the local ions and possibly also to a welding of the contacting grains.

The experimental finding reported here was observed during an attempt to implement this simple concept to YSZ. The observed phenomena will be called flash grain welding (FGW).

A specific experimental difficulty with the oxide ion conductors results from the very nature of their electric current carriers. Because of their ionic nature, they drain with them a certain amount of oxygen, defined by the Faraday law. As sketched in Fig. 1, under DC polarization, at the contact between the sample and the electric current collector negatively polarized,

* Corresponding author. Tel.: +33 619719956.
E-mail address: mikleitz@orange.fr (M. Kleitz).

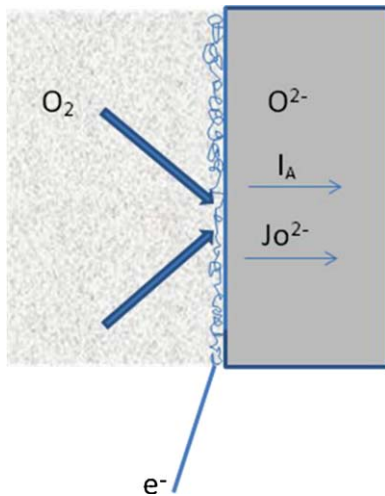
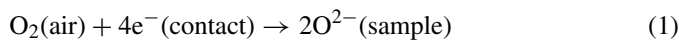


Fig. 1. Sample holder.

the balance of matter shows a deficit of oxygen. This can be compensated by the ions supplied by the so-called electrode reaction:



Numerous experimental results, obtained for instance with fuel cells, show that an efficient compensation cannot be expected for current densities exceeding a few A/cm^2 . When the compensation is not ensured, the sample is chemically reduced. This results in an additional, fairly high, electronic conductivity. This is the so-called blackening process. Experimentally, when this process starts locally, it initiates preferential current routes because of the important local electric resistance fall. It frequently ends in a kind of electrochemical spark through the sample. In the case of yttria stabilized zirconia, the first stage of blackening is reversible, and the material can be re-oxidized without major damage.¹⁶ In the case of ceria, the reduction leads to the formation of large Ce^{3+} ions and to an expansion detrimental to the crystal integrity. In practice, with the high current densities expected to be used in flash welding, higher degrees of blackening are likely to be reached. Then the chemical reduction is no longer reversible. On subsequent re-oxidation, the material is mechanically weakened.

At the other current collector contact, positively polarized, where oxide ions are brought in, the situation is less crucial; excess oxygen simply outgases from the sample. Only under very high current densities, this can physically deteriorate the electric contact.

The conclusion from this sketchy analysis is that AC voltages should preferably be used to investigate the potentialities of the Flash Grain Welding. Passing an alternating current will alternatively re-oxidize the possibly reduced negative electrode sub-layer. To get a quantitative evaluation of the reduction risk, we can simply refer to the Faraday law which relates the oxygen flux $J(\text{O}_2)$ to the electric current I (see Fig. 1):

$$J(\text{O}_2) = \frac{I}{4F} \quad (2)$$

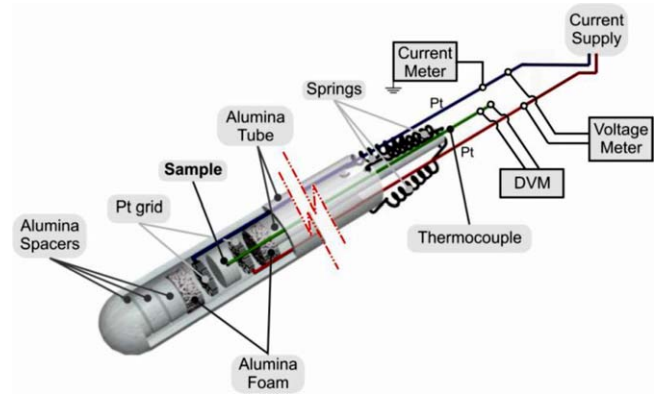


Fig. 2. Fluxes of matter associated with a direct current passing through the sample.

where J is expressed in mol/s and I in A. The Faraday constant F is approximately equal to 96,500 C.

A quantitative application of this equation indicates that each half cycle of a 50 Hz alternating current of $10 \text{ mA}/\text{cm}^2$ drains in and out 0.36 O^{2-} ion per $(5 \text{ \AA})^2$ which is approximately the lateral surface of an elementary YSZ cell.

2. Experimental

Commercial powders (TZ-8Y from Tosoh, Japan) with $75 \mu\text{m}$ average size granules, composed of primary particles of 25 nm mean diameter, were used without further treatment. The samples were pressed, first uniaxially under 46 MPa and then isostatically under 200 MPa. After these pressings, the green relative densities were all close to 50%. To be able to use various equipments, two sets of dimensions were selected. A series of pellets have diameters of the order of 5 mm and a thickness of 3 mm. The other series has 7 mm and 3 mm, respectively. To improve the uniformity of the current distribution through the samples, their bases were covered with Pt paint (Degussa Demetron 308A).

The experimental setup diagram is shown in Fig. 2. The investigated sample is inserted between two current collectors made of either Pt foils or grids. To maintain the electric contact, a slight pressure of a few hundreds grams was ensured by springs and transmitted by an alumina plunger. This sample holder was simply introduced in an electric furnace whose temperature was regulated to within 2°C . All the experiments were performed under air. A thermocouple type S was located close to the sample to qualitatively indicate any heating effect associated with the grain welding.

The impedance analyzer is a Hewlett Packard 4192A run by the Hydro-Quebec impedance spectroscopy software¹⁷ in the 5 Hz to 13 MHz range.

As sources of polarizing current, we used: a DC power supply Tectrol model TCA 30-5; a variable transformer 60 Hz/25 A/220 V simply connected to the main line; a 1 kHz, 60 W home-made power supply.

The sample microstructure was examined in a scanning electron microscope Philips XL30.

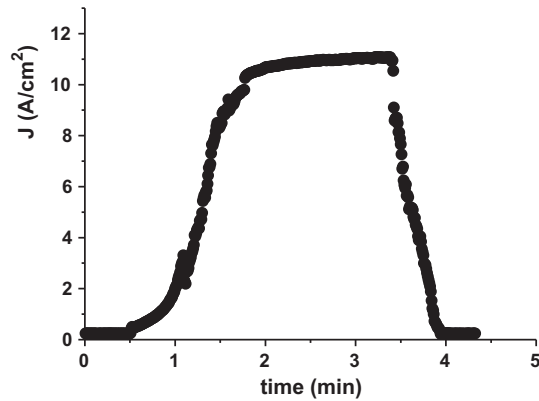


Fig. 3. Typical current versus time variation during a flash grain welding. $T=970^{\circ}\text{C}$; applied voltage 8 V, 1000 Hz; TZ-8Y sample.

The density of the specimen after the FGW experiment was evaluated by the Archimedes method (immersion in water).

3. Results

To evaluate the evolution of the sample electrical resistivity after the Flash Grain Welding, its impedance diagram was systematically recorded at the temperature of treatment before and after the application of the AC welding current.

In essence, the observed phenomenon is summarized in Fig. 3.

In another similar experiment, The initial dimensions were 4.6 mm in diameter and 3.3 mm thick. The experimental temperature was 964°C . At this temperature the initial sample resistance was $270\ \Omega$. An AC voltage of 16 V, 1000 Hz was applied between the current collectors. During $\sim 30\text{ s}$ the recorded current is quasi stable and approximately equal to 60 mA, as expected from the value of the sample resistance. After this elapsed time the current starts increasing abruptly by a factor of 11 during $\sim 30\text{ s}$. Then it levels off and reaches a plateau. On decreasing the applied voltage after the welding, the recorded current shows a behavior approximately ohmic (slightly altered by a Joule heating effect described below, Section 3.3). After returning to the equilibrium temperature of 964°C , the sample resistance shows a decrease by a factor 11. Before the welding, the measured resistance was that of a highly porous material and after it is that of a fairly dense one.

At 420°C , after the welding, the impedance diagram (Fig. 4) has the shape and size of a conventional sintered sample. A deconvolution of this impedance diagram, taking into account the sample geometric factor, gives $5.9\ \text{k}\Omega\ \text{cm}$, $9.2 \times 10^{-12}\ \text{F/cm}$, $2.1\ \text{k}\Omega\ \text{cm}$ and $9.8 \times 10^{-10}\ \text{F/cm}$ for ρ_g , C_g , ρ_{gb} and C_{gb} , respectively. The ρ and C symbols stand for resistivity and specific capacitance for grain (g) and grain boundary (gb), respectively. The measured capacitance values are typical of grain and grain boundary responses.

The sintered sample density determined geometrically and by the Archimedes method is 94% of the theoretical value.

Fig. 5 shows a typical SEM image of its surface microstructure. For this observation, the sample surface was polished with 15 to $1\ \mu\text{m}$ diamond pastes, and thermally etched at 1200°C

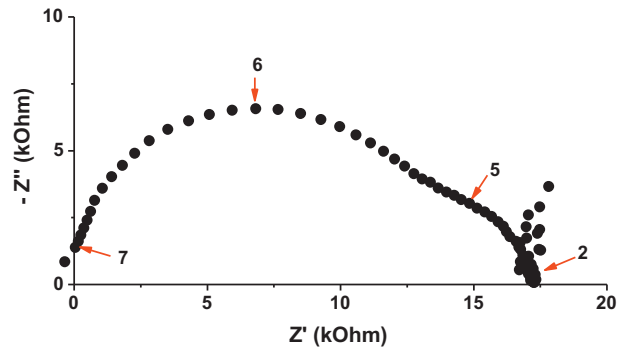


Fig. 4. Impedance spectroscopy diagram of a TZ-8Y sample after flash grain welding at 964°C under 15 V, 1000 Hz. Measurement temperature: 421°C . The numbers stand for the logarithm of the frequency.

for 15 min. The image shows a uniform grain size of the order of 200 nm and pores which are likely to result from imperfect initial compacting. According to the supplier the initial powder mean particle size is 25 nm.

3.1. Current frequency

As expected from the analysis sketched in the introduction, the use of a Direct Current frequently results in sparks through the sample (after the experiment the sample is broken and a black print going from one electrode to the other can be seen). On the other hand, in this first series of measurements, the observed differences between the behaviors under 60 and 1000 Hz are minor. The electric current evolution under 1000 Hz appears smoother with less and smaller oscillations (of the order of a fraction of a second and a maximum amplitude of about 20% of the measured value).

3.2. Initial current density

Quite unambiguously, the determining parameter of the observed phenomena is the initial current density. To arrive at this conclusion, we made two series of measurements. In a first

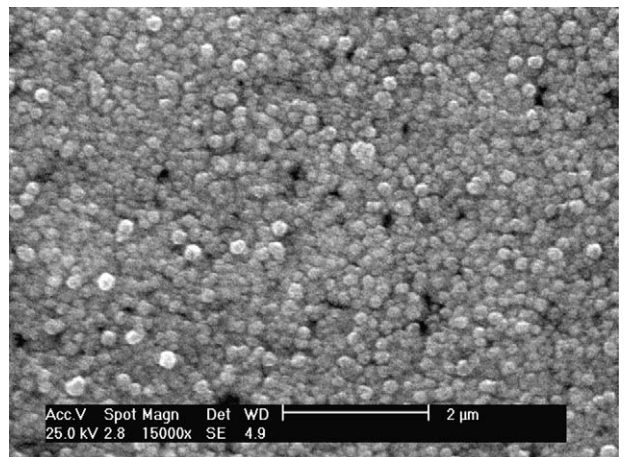


Fig. 5. Scanning electron microscopy image of a polished surface of a TZ-8Y sample after Flash Grain Welding at 964°C under 15 V, 1000 Hz.

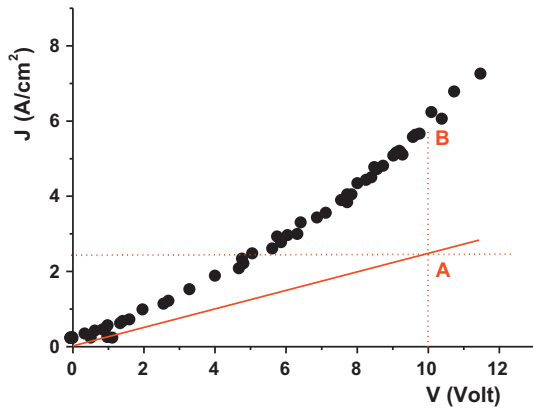


Fig. 6. Current versus applied voltage at 970 °C, after flash grain welding under 15 V, 1000 Hz.

one, we maintained the applied voltage constant (20 V, 1000 Hz) and vary the sample temperature between 700 and 850 °C, thereby varying the sample resistance. In a second one, we maintained the sample temperature constant (970 °C) and therefore its resistance and vary the applied voltage amplitude from 1 to 20 V. In both cases, the avalanche effect was observed for an initial current density higher than approximately 100 mA/cm². For lower initial current densities only small current steps are observed, but without any significant densification, as shown on the impedance diagrams. We could interpret this behavior on the basis of a chain reaction mechanism with threshold. For this we would assume that the grain contacts in the pressed material are distributed according to a “quality parameter” based on their ability to be welded. During a successful welding, the high quality contacts weld first, resulting in a lowering of the sample resistance with a subsequent increase in the current density and, therefore, a welding of the “second” quality contacts, and so on. With a low initial current density, the increase after the first step is not sufficient to activate a chain mechanism.

3.3. Heating effect

After the welding process has occurred, when the current has reached its plateau, the sample is sintered and behave as a regular material, in other words as a simple resistance (taking apart the electrode polarizations which can be reasonably neglected under an AC voltage of 1000 Hz). As in a regular resistance, the passing of a current generates a Joule effect which results in an increase in the sample temperature and therefore in a decrease of its resistance. This is clearly shown in Fig. 6 which presents the $J(V)$ curve recorded on slowly lowering the applied voltage V , after the welding, starting from the current plateau.

The straight line drawn on this figure corresponds to an ideal ohmic behavior without any Joule effect. Its slope is the sample resistance measured under zero current (by impedancimetry). The distance between the two curves, for instance AB in Fig. 6, measures the increase in the current I resulting from the Joule heating of the sample. Referring to the Arrhenius equation of the variation of the sample resistivity with temperature, we can simply use such a measurement to calculate the temperature increase

under the applied voltages, using the following equation.

$$\Delta(\log I) = -\Delta(\log R) = \left(\frac{e}{kT}\right) \cdot \left(\frac{\Delta T}{T^2}\right) \quad (3)$$

where R is the sample resistance, e the resistivity activation energy for YSZ, approximately equal to 1 eV, k the Boltzmann constant and T is the experimental temperature, here 1243 K. In the experiment described in Fig. 6, under 10 V, the calculated temperature increase is 186 °C (the thermocouple located close to the sample and seen in Fig. 2 showed a temperature increase of about 25 °C). The temperature increases, calculated in this way, added to the furnace temperature which is, for instance 970 °C, give maximum sample temperatures during the welding of the order of 1150 °C, far below the “conventional” fast sintering temperatures. Furthermore, at the start of the welding process, before the current step (Fig. 3), the current density is significantly lower, typically by a factor of 10. Then, the Joule effect and the temperature increase are therefore likely to be significantly lower.

From this analysis we can conclude that the observed welding effect cannot be due to a simple overall Joule heating of the sample.

4. Conclusions

The phenomenon we have observed is a fast sintering which does not require any pressure. It is induced by a passing of an alternating current through a pre-pressed sample. At this level of investigation, it appears that a minimum current density has to be overcome to start the process. The technique which implements it, is very simple and can be applied to self-standing samples. No costly equipment is required.

The reported numerical data may appear somewhat scattered, inaccurate. We rapidly performed some 25 experiments on various materials, sometimes including different series of measurements. We search to highlight the main features of the phenomenon and to select appropriate experimental conditions. The reported data have been selected to allow the reader to easily repeat the experiment and observe the phenomenon without going through tedious trial and error experiments.

This phenomenon is fairly similar to the observation made by Cologna et al.¹³ during an investigation of the effect of an applied DC voltage on the sintering kinetic of a nanograined TZP. However, according to our results, the use of a Direct Current described by these authors is likely to give a poor yield.

Acknowledgements

M. Kleitz expresses his gratitude to FAPESP for providing the Fellowship Grant no. 2010/51293-0. The authors acknowledge the contribution of Y. Miyao, who designed and assembled the 1000 Hz power supply used in this study.

References

1. Munir ZA, Anselmi-Tamburini U, Ohyanagi M. The effect of electric field and pressure on the synthesis and consolidation of materials: a review of the spark plasma sintering method. *J Mater Sci* 2006;**41**:763–77.
2. Orru R, Licheri R, Locci AM, Cincotti A, Cao G. Consolidation/synthesis of materials by electric current activated/assisted sintering. *Mater Sci Eng R-Rep* 2009;**63**:127–287.
3. Grasso S, Sakka Y, Maizza G. Electric current activated/assisted sintering (ECAS): a review of patents 1906–2008. *Sci Technol Adv Mater* 2009;**10**:1–24.
4. Garay JE. Current-activated, pressure-assisted densification of materials. *Annu Rev Mater Res* 2010;**40**:445–67.
5. Munir ZA, Quach DV, Ohyanagi M. Electric current activation of sintering: a review of the pulsed current sintering process. *J Am Ceram Soc* 2011;**94**:1–19.
6. Anselmi-Tamburini U, Garay JE, Munir ZA. Fast low-temperature consolidation of bulk nanometric ceramic materials. *Scr Mater* 2006;**54**:823–82.
7. Anselmi-Tamburini U, Woolman JN, Munir ZA. Transparent nanometric cubic and tetragonal zirconia obtained by high-pressure pulsed electric current sintering. *Adv Funct Mater* 2007;**17**:3267–73.
8. Yang D, Conrad H. Influence of an electric field on the superplastic deformation of 3Y-TZP. *Scr Mater* 1997;**36**:1431–5.
9. Starnes S, Conrad H. Grain size distribution in ultrafine-grained yttria-stabilized zirconia deformed without and with an electric field. *Scr Mater* 2008;**59**:1115–8.
10. Ghosh S, Chokshi AH, Lee P, Raj RA. Huge effect of weak dc electrical fields on grain growth in zirconia. *J Am Ceram Soc* 2009;**92**:1856–9.
11. Yang D, Conrad H. Enhanced sintering rate of zirconia (3Y-TZP) by application of a small AC electric field. *Scr Mater* 2010;**63**:328–31.
12. Cologna M, Raj R. Surface diffusion-controlled neck growth kinetics in early stage sintering of zirconia, with and without applied DC electrical field. *J Am Ceram Soc* 2010;**93**:3556–9.
13. Cologna M, Rashkova B, Raj R. Flash sintering of nanograin zirconia in <5 s at 850 °C. *J Am Ceram Soc* 2010;**93**:3556–9.
14. Dessemond L, Kleitz M. Effects of mechanical damage on the electrical properties of zirconia ceramics. *J Eur Ceram Soc* 1992;**9**:35–9.
15. Steil MC, Thevenot F, Kleitz M. Densification of yttria stabilized zirconia. Impedance spectroscopy analysis. *J Electrochem Soc* 1997;**144**:390–8.
16. Fouletier J, Kleitz M. Electrically renewable and controllable oxygen getter. *Vacuum* 1975;**25**:307–14.
17. Kleitz M, Kennedy JH. Resolution of multicomponent impedance diagrams. In: Vashishta P, Mundy JN, Shenoy GK, editors. *Fast ion transport in solids*. The Netherlands: Elsevier/North-Holland; 1979. p. 185.